Brain Structure and Function (2019) 224:627–642
https://doi.org/10.1007/s00429-018-1797-8

ORIGINAL ARTICLE

Knockdown of calcium-binding *calb2a* and *calb2b* genes indicates the key regulator of the early development of the zebrafish, *Danio rerio*

Rahul C. Bhoyar[1] · Arun G. Jadhao[1] · Ankit Sabharwal[2] · Gyan Ranjan[4] · Sridhar Sivasubbu[2] · Claudia Pinelli[3]

Received: 16 June 2018 / Accepted: 15 November 2018 / Published online: 20 November 2018

Abstract

The present study initiates our investigation regarding the role of *calb2a* and *calb2b* genes that are expressed in the central nervous system, including the multiple tissues during early embryonic development of zebrafish. In this study, we have adopted individual and combined morpholino-mediated inactivation approach to investigate the functions of *calb2a* and *calb2b* in early development of the zebrafish. We have found that *calb2a* and *calb2b* morpholino alone failed to generate an obvious phenotype; however, morphological inspection in early developmental stages of *calb2a* and *calb2b* combined knockdown morphants show abnormal neural plate folding in midbrain-hindbrain region. In addition to this, combinatorial loss of these mRNA leads to severe hydrocephalus, axial curvature defect, and yolk sac edema in later developmental stages. Also, the combined knockdown of *calb2a* and *calb2b* are found to be associated with an impaired touchdown and swimming performance in the zebrafish. Co-injection of the *calb2a* and *calb2b* morpholino oligonucleotide cocktail with human *CALB2* mRNA leads to the rescue of the strong phenotype. This study provided the first comprehensive analyses of the zebrafish Calb2a and Calb2b proteins; we have found that Calb2a and Calb2b are highly conserved across vertebrate species and originated from the same ancestral gene long back in the evolution. Homology modeling and docking with the similar structure and Ca^{2+} binding sites for both proteins provide the evidence that both the proteins may have similar function and one can compensate for the loss of other. Collectively, these findings confirm the unique and essential functions of *calb2a* and *calb2b* genes in the early development of the zebrafish.

Keywords *Calb2a* · *Calb2b* · Calcium-binding proteins · Midbrain-hindbrain boundary · Zebrafish

Abbreviations

Calb2a	Calbindin 2a
Calb2b	Calbindin 2b
CALB2	Calbindin 2
CaBPs	Calcium-binding proteins
PV	Parvalbumin
MO	Morpholino oligonucleotide
NIC	Non-injected control
CNS	Central nervous system
hpf	Hours post fertilization
dpf	Day post fertilization
MHB	Midbrain-hindbrain boundary
Tg	Tegmentum
Hb	Hindbrain
nL	Nanolitre
mM	Millimolar
mm	Millimetre
pg	Picogram
PTU	*N*-phenylthiourea

Electronic supplementary material The online version of this article (https://doi.org/10.1007/s00429-018-1797-8) contains supplementary material, which is available to authorized users.

✉ Arun G. Jadhao
agj213@hotmail.com

[1] Department of Zoology, RTM Nagpur University, Nagpur 440033, India

[2] Zebrafish Functional Genomics, CSIR Institute of Genomics and Integrative Biology, New Delhi, India

[3] Department of Environmental, Biological and Pharmaceutical Sciences and Technologies, University of Campania "Luigi Vanvitelli", 81100 Caserta, Italy

[4] Department of Genetic Engineering, Kattankulathur Campus, SRM Institute of Science and Technology, Chennai, Tamil Nadu 603203, India

pdb Protein database
BLAST Basic Local Alignment Search Tool

Introduction

Calcium-binding proteins (CaBPs) Calbindin 2a (Calb2a, previously known as calb2 or calretinin) and its closely related paralog calbindin 2b (Calb2b, previously known as calbindin 2-like), are the proteins that belong to EF-hand family of the CaBPs and are well conserved across the species (Persechini et al. 1989; Heizmann and Hunzlker 1991; Baimbridge et al. 1992; Andressen et al. 1993; Yokoi et al. 2009). The name "EF-hand" is derived from the spatial orientation of the fifth (E) and sixth (F) -helix of parvalbumin (Pv), which together with a metal-binding loop of 12 amino acids form this evolutionary well-conserved metal-binding motif have the high affinity calcium-binding site (Moews and Kretsinger 1995).

Calb2a and Calb2b are the high-affinity calcium-binding proteins belonging to the calmodulin superfamily, which plays an important role in calcium uptake as mediator of transcellular calcium transport and calcioprotection in several distinct types of neurons (Bronner 1990; Berdal et al. 1991; Nemere et al. 1991; Lledo et al. 1992; Roberts 1993; Chard et al. 1993). The Calb2a and Calb2b immunoreactivity has been well studied in central nervous system (CNS) of different vertebrate groups including fish. The immunocytochemical studies of these two proteins show their expression in the CNS intestine, kidney and pancreas of higher classes, viz. amphibians and birds (Christakos et al. 1979; Jande et al. 1981a, b; Baimbridge and Miller 1982; Jadhao and Malz 2007; Jadhao and Deshpande 2014; Deshpande and Jadhao 2015). The immunoreactivity of the Calb2a been demonstrated experimentally in the CNS and peripheral nervous system (PNS) of adult zebrafish (Castro et al. 2006; Levanti et al. 2007). In our recent study we have demonstrated the gene expression of these two calcium-binding proteins in CNS and PNS during the early embryonic development of the zebrafish using the whole mount in situ hybridization study (Bhoyar et al. 2017).

These two proteins are closely related and display 58% of the homology at the level of the amino acid sequence. Phylogenetic analysis of *calb2a* and *calb2b* shows that these two genes are co-orthologs of tetrapod *Calb2* and thought to be emerged in the genome duplication that preceded the teleost radiation (Amores et al. 1998; Postlethwait et al. 1998; Jaillon et al. 2004; Yokoi et al. 2009). In our previous study, a high level of *calb2a* and *calb2b* mRNA expression was detected in the eye, brain, spinal cord and other tissues at various developmental stages of zebrafish, thus leading to the conclusion that both the genes may play an important role in early development of these tissues in the fish (Levanti et al. 2007).

To further prove the role of these genes in early embryonic development, zebrafish (*Danio rerio*) is used as the model organism due to its important characteristics which include high fecundity to produce the large embryos that are optically transparent which means organs, cells and tissues are visualized in vivo and exact development process can study in real-time (Fishman 1999), rapid development, the entire body plan established by 24 h post fertilization (hpf) and most of the internal organs totally developed by 96 hpf (Westerfield 2007). These characteristics of zebrafish facilitate the researcher to study the early development processes and makes the zebrafish an excellent model system for studying early vertebrate development.

Morpholino oligonucleotides (MOs) are the most acknowledged gene-specific antisense knockdown technology used in many model systems including zebrafish. Morpholinos have been used to accelerate gene discovery through large-scale screening (Pickart et al. 2006; Eckfeldt et al. 2005) to study the function of the specific gene (Lanet al. 2007) and to authenticate mutant phenotypes (Nasevicius and Ekker 2000). Two types of MOs are used in zebrafish including translational blocking which binds to complementary mRNA sequences within the 5′ untranslated region (UTR) near the translational start site hindering ribosome assembly and further translation of mRNA (Summerton 1999) and splice blocking MO, thought to be binding and inhibiting pre-mRNA processing via inhibition of the spliceosome components (Morcos 2007). The present study is aimed at understanding the role of these two closely related genes in the early embryonic development of the zebrafish using splice blocking MO-based combined knockdown of *calb2a* and *calb2b* genes.

Materials and methods

Ethics statement

All zebrafish work was carried out with the recommendations and guidelines stipulated by the CSIR, Institute of Genomics and Integrative Biology, Government of India. The protocol was approved by the Institutional Animal Ethics Committee (IAEC) of the CSIR Institute of Genomics and Integrative Biology, Government of India. Care was taken to minimize the numbers of animals used in these experiments.

Zebrafish maintenance and breeding

Wild-type zebrafish of the ASWT (Patowary et al. 2013) strain were housed and maintained in a circulating tank

system (Aquaneering, SanDiego, CA) at CSIR-Institute of Genomics and Integrative Biology as per standard practices (Westerfield 2000). Embryos were obtained by natural spawning and cultured at 28.5 °C in embryo water (0.1 g/L Instant Ocean Sea Salts, 0.1 g/L sodium bicarbonate, 0.19 g/L calcium sulphate, 0.2 mg/L methylene blue, H2O). The developmental stages of the embryos were determined by the hours post fertilization (hpf) and by morphological features, as described by Kimmel et al. embryo water was supplemented with 200 mM (0.003%) PTU (N-phenylthiourea, Sigma Aldrich) to prevent pigment formation (Karlsson et al. 2001).

Identification and sequence retrieval of Calb2a and Calb2b

Sequences of Calb2a and Calb2b proteins of zebrafish were retrieved from Uniprot (Q6PC56/Q6PC44) (UniProt Consortium 2016). The sequence was aligned with human, mouse, rat, bovine and chick using cluster omega (Sievers et al. 2011) and visualized in Mview (Brown et al. 1998). A phylogenetic tree was constructed by neighbor-joining method and was visualized using interactive Tree Of Life (iTOL) (Letunic and Bork 2016).

Morpholino oligonucleotide design

The *calb2a* and *calb2b* splice-blocking morpholinos oligonucleotides were designed and obtained from Gene Tools, LLC, as suggested by the manufacturer (Gene Tools, LLC). The *calb2a* splice blocking MO (5′-TGATTGTTCCTCTAT ACCTCTGACA-3′ *calb2a* MO) including 5-mispair oligo (5′-TGAaTcTTCgTCTATACCTgTcACA-3′) as specificity controls was designed at exon 3 of *calb2a* pre-mRNA (AGA ATTGAGA [TGTCAGAGgtatagaggaacaatca]tttaacac). The *calb2b* splice blocking MO (5′-GCACAAAATTCATGA CTCACCGCAG-3′) was constructed on Exon 2 of *calb2b* pre-mRNA (GGAAAA[CTGCGgtgagtcatgaattttgtgc]gtcga). Both the morpholinos oligonucleotides were obtained as lyophilized forms were dissolved in 300 µL of nuclease-free water (NFW) to get the final concentration of 1 mM.

Morpholino injections

A cocktail of the *calb2a* MO and *calb2b* MO was prepared with following different concentrations: 0.5 mM, 0.4 mM, 0.3 mM, 0.2 mM. Zebrafish embryos were collected within 15 min of spawning and were placed on cooled agarose loading plates (Westerfield 2000; Hermanson et al. 2004). The needles used in microinjection were made by pulling the glass capillaries in a Sutter P-87 instrument (Hyatt and Ekker 1999). The needle was back loaded with 2–3 Microliter (µL) of morpholino solution by using microloader pipet tips (Eppendorf). Before injection, the needle was calibrated using the Harvard Apparatus (PLI 90) Pico-injector to regulate the drop size. The Pico-injector was set for the defined time pulse, and the needle tip was clipped with the help of the Dumont no. 5 watchmaker forceps to create an aperture. Drop size was tested after each break until the desired calibration was achieved. After opening the end of the needle, drop solution was transferred to a microcapillary (Drummond) to measure the drop volume. The microcapillary tube holds approximately 30 nL in 1 mm. The needle tip was clipped until the drop reaches the desired volume of 1 mM. The pico-injector controls were set for a 100-millisecond (ms) pulse to obtain the 3-nL drop size. This method of calibration provides the consistency in the volume of morpholino solution in every injection. Embryos were injected at the one-cell stage with different concentrations of 0.5 mM, 0.4 mM, 0.3 mM and 0.2 mM/3 nL volume of cocktail morpholino solution and with 0.4 mM of the 5-mispair specificity control MO. Injected embryos were allowed to recover in system water at 28.5 °C to 50% epiboly (5–6 h). The injected embryos were screened after 6 hpf for percent survivability. Embryos were later transferred to embryo water supplemented with 200 mM (0.003%) PTU (*N*-phenylthiourea, Sigma Aldrich) at 28.5 °C for further development.

Screening and imaging

Dead or undeveloped embryos were removed daily; injected embryos were screened for neural tube folding abnormalities along with any developmental defect on the following day around 24 h. We have used the 24-h time point for screening the brain development defects since it allows us to better distinguish between the normal and the injected phenotypes. Embryos showing the positive phenotypes were screened and photographed at different developmental time points using Trinocular Stereozoom Microscope SMZ 800N Nikon.

Touch-response assay

To gain insight into how the combined loss of *calb2a* and *calb2b* alters the behavior and swimming performance, we performed the following experiment: The combined *calb2a* and *calb2b* mutant phenotypes along with the NIC zebrafish larvae of 5 dpf development stages were placed individually into the chambers of 12-well plates containing embryo water. Touch-evoked behaviors were elicited by touching a trunk or tail of larvae with a microloader pipet tip. Behavioral

touch responses were assessed with Trinocular Stereozoom Microscope SMZ 800N Nikon.

Semi-quantitative RT-PCR to validate *calb2a* and *calb2b* knockdown

Total RNA was isolated from 40 embryos or larvae from screened morphants of different MO concentrations along with the control zebrafish embryos of the same stage using TRIzol reagent (Invitrogen) followed by TURBO™ DNase treatment according to standard protocols (Life Technologies). For cDNA synthesis, 1 µg of RNA was reverse transcribed using the SuperScript III™ First-Strand Synthesis System (Life Technologies). A cDNA was then used as a template for PCR to test for mis-splicing events induced by the *calb2a* and *calb2b* slice blocking MOs. The primer pairs spanning each exon/intron boundary was constructed to check the intron retention [*calb2a* (forward) 5′-GATCCC TCAAATGCAGCCTT-3′, (reverse) 5′-ATGAATTCGGTG CTGGATCC-3′ *calb2b* (forward) 5′-GCTGCATTGAAG GGAAGGAA-3′, (reverse) 5′-ATCTTCCCATCACCGTTC TC-3′]. A PCR amplified products were electrophoresed on a 1.5% agarose ethidium bromide gel and checked for banding patterns and relative band intensities.

Human *CALB2* mRNA synthesis and microinjection

PCR reaction was conducted using a pair of (forward-5′TGA GGTCTCCGAGCGGCT3′ and reverse-5′AGGTGTGTG CAGGCTGTA3′) primers which amplify the human *CALB2* full coding sequence using cDNA as the template. The PCR amplified *CALB2* products were cloned into TOPO-TA 2.1 Vector (Invitrogen) and linearized using enzyme SpeI (NEB); the linearized plasmid was purified, and the purified plasmid was used to transcribe the full-length *CALB2* mRNA. A capped mRNA was prepared using mMESSAGE mMACHINE® SP6 Kit (Ambion) as per the manufacturer's instruction. Stocks of synthetic *CALB2* mRNA solutions were quantified by recording absorbance at 260 and 282 nm and diluted to the desired concentrations in RNase-free water for microinjection. The 250 pg of *CALB2* full-length mRNA was co-injected with 0.4 mM cocktail of *calb2a* and *calb2b* MO; the injected embryos were incubated for 24 h at the controlled temperature and were examined for the effect of the injected *CALB2* mRNA.

Homology protein modeling, docking and functional prediction

Templates for generating homology models were selected using BLAST (Basic Local Alignment Search Tool) search against protein database (pdb) option (Altschul et al. 1997; Berman et al. 2000). Selected templates with high sequence identity and low e-value belonging to same protein family were used to generate homology model using molecular modeling GUI platform—EasyModeller 4.0 which runs on MODELLER program (Kuntal et al. 2010; Webb and Andrej 2014). Also, SWISS-MODEL and I-TASSER (Iterative Threading ASSEmbly Refinement) servers were used for generating the homology model for Calb2a and Calb2b proteins (Schwede et al. 2003; Zhang 2008). We have generated 20 models for Calb2a (EasyModeller 4.0-12; SWISS-MODEL- 6; I-TASSER- 2) and 19 models for Calb2b (EasyModeller 4.0-12; SWISS-MODEL-6; I-TASSER-1). Model validation was performed using Ramachandran (RC)-plot (by RAMPAGE), ERRAT2 plot, Verify 3D, Dope score and Q-MEAN score. We also have calculated RMSD (root-mean- square deviation) of the models with (PDB id) 2G9B as it belongs to calbindin of *Rattus norvegicus*. Top one model was selected from Calb2a and Calb2b each and was further used in docking (Lüthy et al. 1992; Colovos and Yeates 1993; Lovell et al. 2003; Benkert et al. 2008).

STRING (*Search Tool for the Retrieval of Interacting Genes/Proteins*) server was used to predict the protein–protein interaction of Calb2a and Calb2b individually and a protein interaction network was constructed by it (Szklarczyk et al. 2015).

The docking was performed using COACH server—which uses TM-SITE and S-SITE relative techniques to predict the binding domains for the selected model (Yang et al. 2013a, b). The top predicted site was selected based on the confidence score of the prediction. It was further visualized using Chimera and Pymol. The hydrogen bond interaction of the Ca^{2+} with the protein was analyzed using Lig-plot software (Wallace et al. 1995). The MIB: Metal Ion-Binding Site Prediction and Docking Server (Lin et al. 2016) was further used to support the predicted Ca^{2+} binding site.

Data analysis and plates preparation

After knockdown of the *calb2a* and *calb2b* mRNA, the injected zebrafish embryos were screened and imaged using an upright Zeiss Axioscope 40 microscope (Carl Zeiss, Germany). Images were taken in white light exposures; the brightness and contrasts of the images were adjusted using Adobe Photoshop version 7.0 and photoplates were made using Corel Draw version X7.

Results

CALB2 is highly conserved across the different species

The phylogenetic analysis reveals that CALB2 is highly conserved across vertebrate species and has originated from the

same ancestral gene long back in evolution. In zebrafish, two copies of the CALB2 are present, i.e., *calb2a* and *calb2b*, which can be due to duplication of the gene at early node as shown in the phylogenetic tree (Fig. 1a). We also performed multiple sequence alignment and observed that most of the vertebrate has > 70% amino acid sequence identity (Fig. 1b). According to the percent identity matrix zebrafish Calb2a and Calb2b shows 80.67% sequence homology with the highly conserved amino acid sequence. When compared with the human and zebrafish, Calb2a shows 76.75% and Calb2b shows 77.12% sequence homology, respectively. These results collectively indicate strong conservation of the CALB2 protein coding sequence across the species.

Phenotypic characterization of *calb2a* and *calb2b* combined knockdown morphant

Embryos injected with different doses of *calb2a* and *calb2b* cocktail MO solutions (0.5 millimolar (mM), 0.4 mM, 0.3 mM, 0.2 mM) show a remarkable reduction in the level of mRNA expression. At lower i.e., 0.2 mM concentration MO injection fail to generate any notable phenotypes. However, at 0.5 mM concentration, the lethality along with the phenotypes generated was beyond the acceptance level, due to this both the concentrations were eliminated for the further study. The *calb2a* and *calb2b* MO cocktail of the concentrations 0.4 mM, 0.3 mM shows a higher phenotypic penetrance along with the more than 50% survival rate (Fig. 2). Several phenotypes were consistently observed in the 0.4 mM, 0.3 mM dose injected morphants along the with decrease in the overall size and length of the *calb2a* and *calb2b* morphants at fixed time points compared with non-injected control (NIC) siblings. To determine whether the difference in size was due to a general developmental delay or injected morpholino, we stage-matched morphant and control embryos according to somite number at 14 hpf and compared morphology between 24 and 72 hpf. This finding ruled out the general

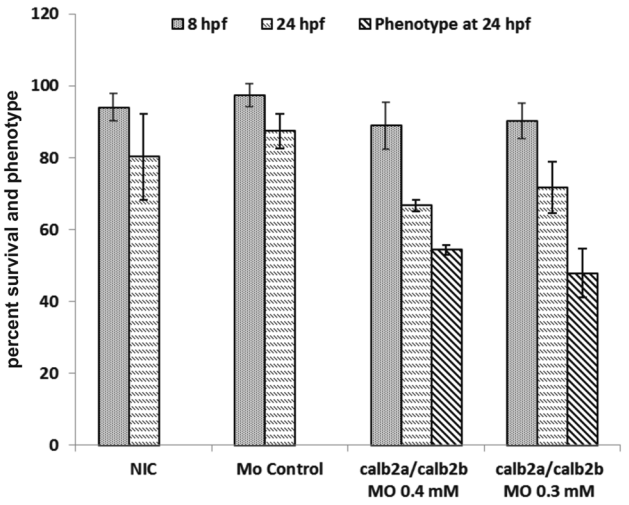

Fig. 2 Graph showing the survival and phenotype percentage of the *calb2a* and *calb2b* cocktail injected zebrafish embryos

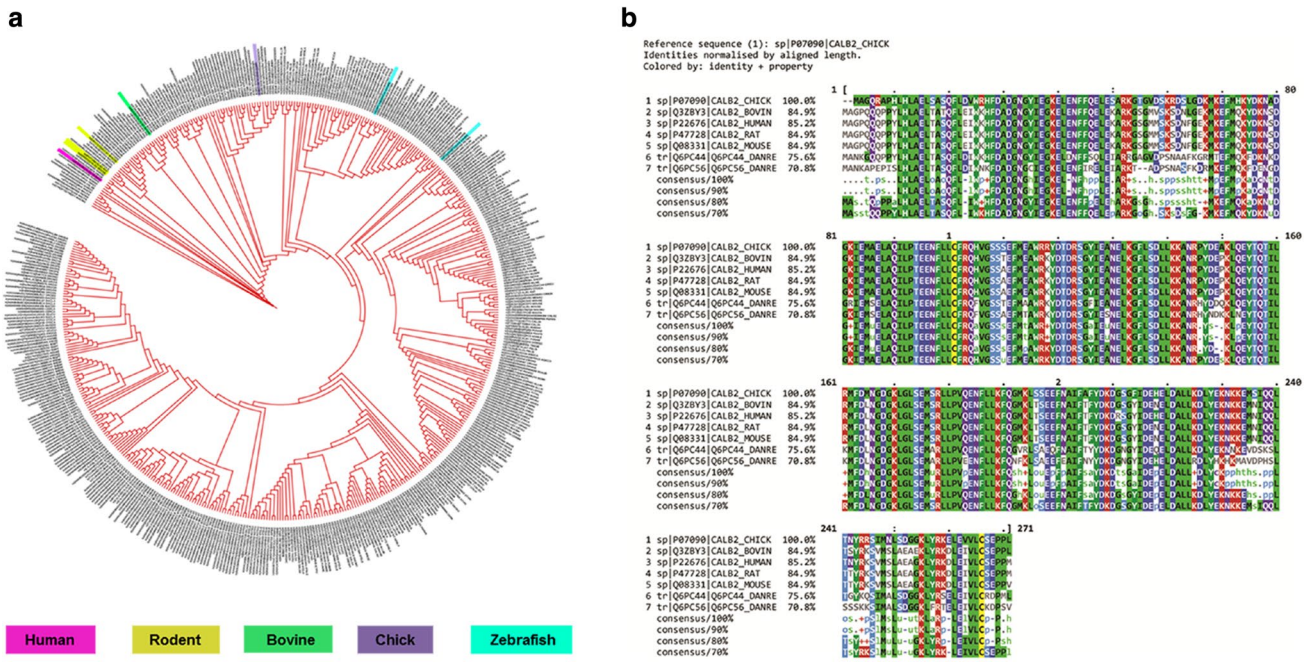

Fig. 1 **a** Phylogenetic tree analysis showing duplication of Calb2 during evolution. **b** Multiple sequence analysis of human, rodent, zebrafish, bovine and chick showing highly conserved protein sequence

developmental delay phenotypes and proved the delay was due to the injected morpholino.

Combined knockdown of *calb2a* and *calb2b* affect midbrain–hindbrain boundary formation

Our Previous study of *calb2a* and *calb2b* mRNA expression during early embryonic development of the zebrafish shows very high mRNA expression in the tegmentum (Tg), midbrain-hindbrain boundary (MHB), hindbrain (Hb) in the developing zebrafish embryos (Bhoyar et al. 2017), suggesting its possible role in zebrafish neural development. Further to understand the role of *calb2a* and *calb2b* gene in early embryonic brain development, we have knockdown these two genes by using splice-blocking morpholino. The MO at concentrations of 0.3 mM and 0.4 mM/3 nL was microinjected into the yolk of one-cell stage zebrafish embryos, control embryos were injected with 0.4 mM of control MO and the brain morphology of the *calb2a* and *calb2b* combined knockdown morphant zebrafish embryos were examined at 24 and 30 hpf of development with dissecting stereo microscopes. At these stages, the size and shape of telencephalon, diencephalon, tectum, tegmentum, midbrain-hindbrain boundary, hindbrain and brain ventricles can be easily scored. Morphological inspection in early development stages of *calb2a* and *calb2b* knockdown morphants shows abnormal neural plate folding in MHB region when compared with the NIC and control MO injected embryos at 24 and 30 hpf stages. The nature of the abnormality in the furrow which separates midbrain from hindbrain varied with the concentration of the MO solution injected. Smaller concentration (0.3 mM) leads to a partially organized MHB boundary, whereas the embryos that were injected with 0.4 mM concentration failed to form the midbrain-hindbrain region (Figs. 3, 4).

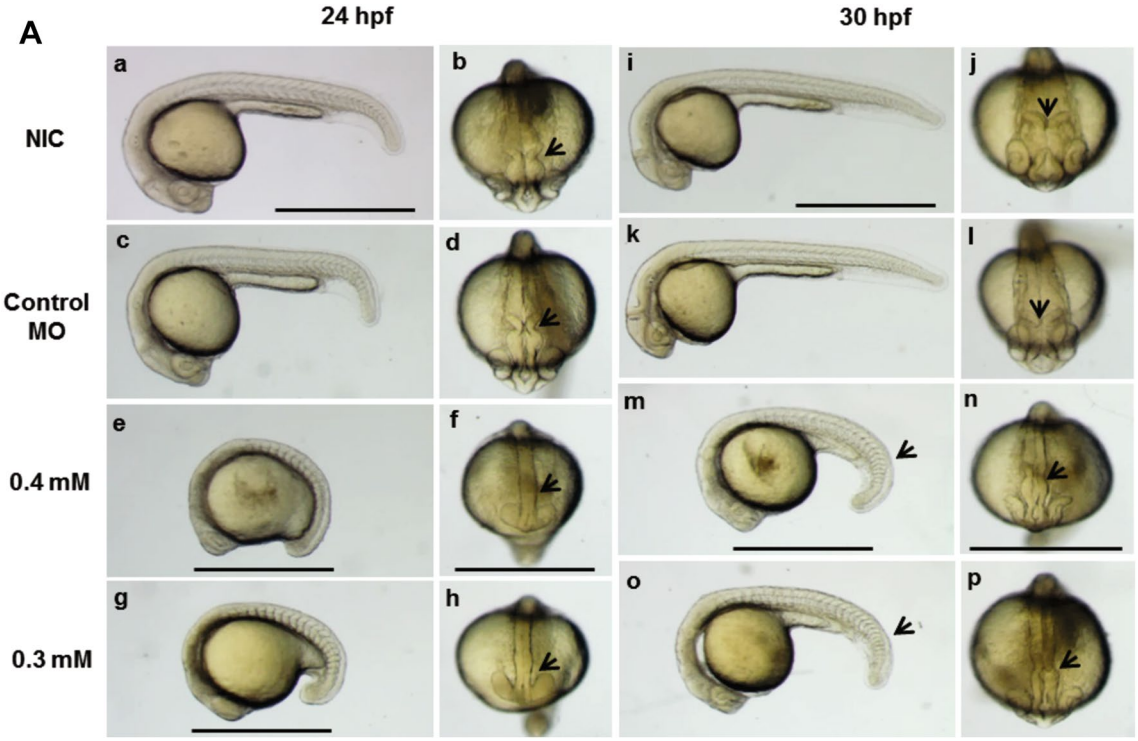

Fig. 3 **A** Phenotypes of zebrafish embryos injected with morpholino oligonucleotides (MO) targeting *calb2a* and *calb2b* mRNA. Zebrafish embryos were injected with 0.4 Millimolar (mM) 0.3 mM of *calb2a* and *calb2b* MO cocktail solution along with the 5-mispair control morpholino as indicated and screened at 24 hpf and 30 hpf. Lateral and dorsal view of 24 h post fertilized (hpf) zebrafish embryos, **a, b** non-injected control (NIC) zebrafish embryos. **c, d** Control MO-injected embryos, **e, f** 0.4 mM cocktail injected embryos, **g, h** 0.3 mM MO injected morphants, arrowhead indicating the defect in neural tube folding in injected embryos when compared with the NIC embryos (**a, b**). 30 hpf zebrafish embryos, **i, j** NIC zebrafish embryos, **k, l** control MO-injected embryos, **m, n** 0.4 mM cocktail injected, **o, p** 0.3 mM cocktail injected morphants arrowhead indicating the defect in neural tube folding, small head and bent tail phenotype. **B** 52 hpf zebrafish embryos, **q, r** NIC embryos, **s, t** control MO-injected embryos **u, v** 0.4 mM cocktail injected, **w, x** 0.3 mM cocktail injected morphants, arrowhead showing the phenotypes of axial curvature and severe hydrocephalus (line). **y**–**f′** 72 hpf zebrafish embryos, **y, z** NIC embryos, **a′, b′** control MO-injected embryos, **c′, d′** 0.4 mM cocktail injected, **e′, f′** 0.3 mM cocktail injected. Morphants with the axial curvature (arrowhead), small head (arrowhead), and severe hydrocephalus (star) yolk sac edema (line) was observed. Scale bar 1 mm

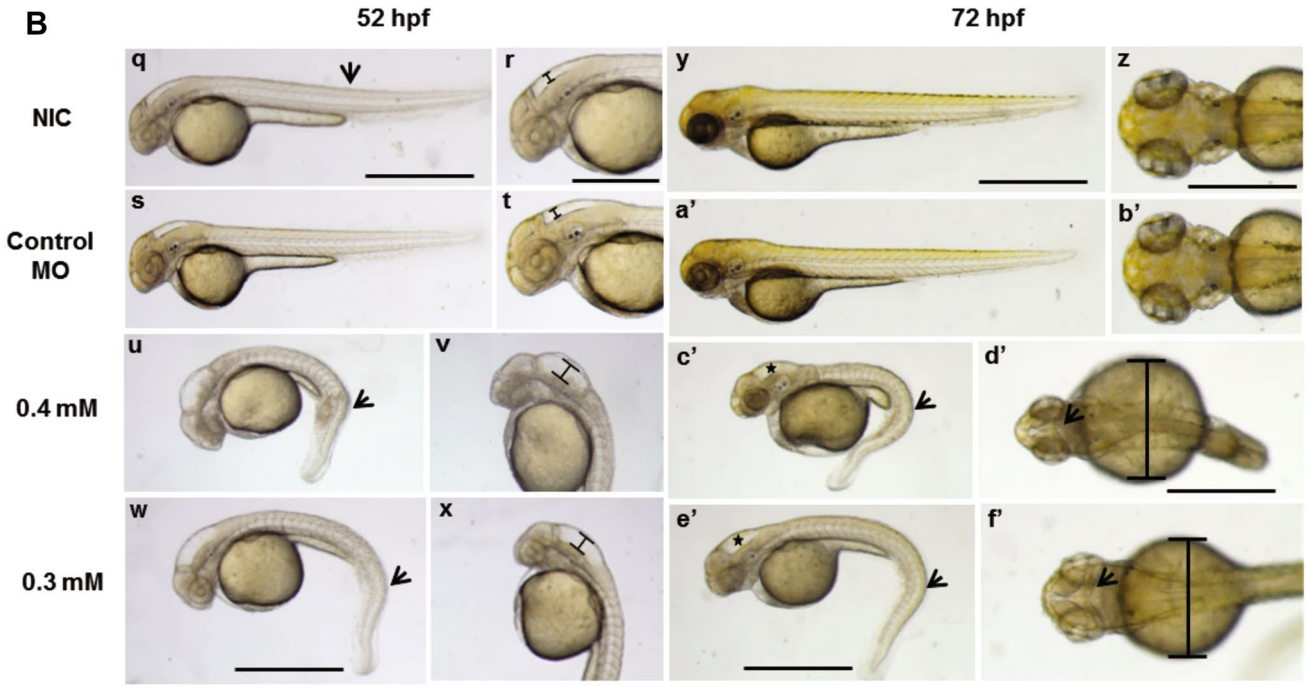

Fig. 3 (continued)

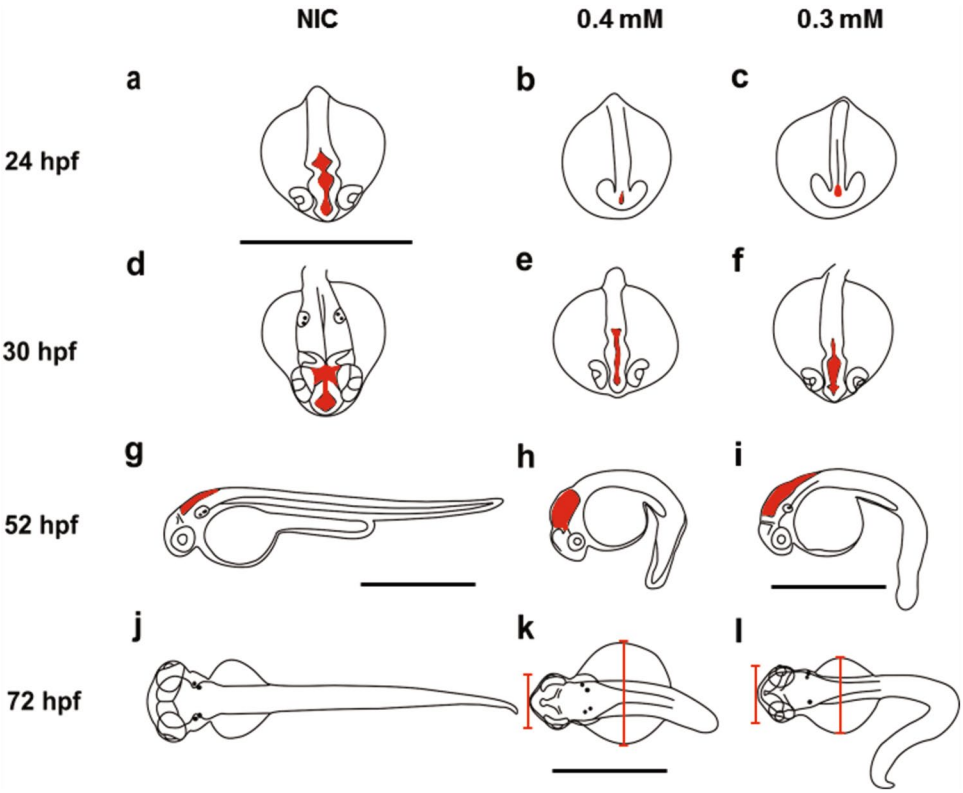

Fig. 4 Schematic representation of the combined *calb2a* and *calb2b* knockdown zebrafish embryos (**a**–**f**) altered brain ventricle morphology resulted in the disorganized Midbrain-hindbrain boundary (MHB) formation (denoted by the red color) in the *calb2a* and *calb2b* morphant embryos compared with non-injected control (NIC) embryos. **g**–**i** Morphant fish displaying hydrocephalus (red color) and curly-tail phenotype compared to unaffected siblings. **j**–**l** schematic view of phenotypes of combined MO-injected zebrafish embryos at 72 hpf showing small head and severe yolk sac edema

Combined Knockdown of *calb2a* and *calb2b* leads to severe hydrocephalus, axial curvature defect and yolk sac edema

The most striking phenotype in the *calb2a* and *calb2b* morphants, involved pronounced hydrocephalus in the midbrain and hindbrain ventricles compared with wild-type embryos and the embryos injected with the control MO (Fig. 3q–f'). This phenotype could be observed as early as 36 hpf and became more provable at 52 hpf. A greater phenotypic penetrance was noted at a higher dose (0.4 mM) with severe hydrocephalus. However, the same phenotype with mild hydrocephalus was also observed at lower MO concentration (0.3 mM).These phenotypes were consistently observed almost all *calb2a* and *calb2b* combined morphants (Figs. 3, 4). In addition to this brain ventricle phenotype, *calb2a* and *calb2b* combined knockdown morphant zebrafish also displayed phenotypes with 'curly tail down' (Figs. 3, 4). A sickle-shaped body or 'curly tail down' is the most frequently observed phenotype, first observed at 24 hpf and by 3 days post fertilization (dpf) all the morphants shows a strong downward curve in their body axis, which is known characteristic of mutants with defects of early CNS development (Brand et al. 1996). We have taken a follow up of these listed phenotypes to 5 dpf, we found that there was a significant recovery in hydrocephalus and yolk sac edema, however, the axial curvature defect was not recovered at this point and embryos were still showing 'curly tail down' phenotype with no effect on mortality rate. These observations suggest that combined loss of *calb2a* and *calb2b* during the early embryonic development of zebrafish produces the permanent defect in axial curvature.

Knockdown of *calb2a* and *calb2b* resulted in the impaired touchdown and swimming performance

Touchdown and swimming performance of *calb2a* and *calb2b* knockdown morphants and live swimming of NIC wild-type embryos were examined by video microscopy with a touch-evoked escape behavior assay at 5 dpf development point. At this stage, wild-type NIC larvae were active; and show the response to tactile stimuli. NIC group larvae were able to swim away from the direction of the applied stimuli (Movie-1). Compared with the NIC, morphant larvae were not active, and they either fail to respond to the applied stimuli or shows corkscrew-like swimming path (Movie-2).

Knockdown of *calb2a* and *calb2b* leads to aberrant intron retention

The *calb2a* and *calb2b* MOs were injected into one-cell stage embryos, in order to determine whether splicing was affected in the morphants, we analyzed mRNA size across exons III–IV and exon II-III in the *calb2a* and *calb2b* gene respectively, using reverse transcription (RT)-PCR. The *calb2a* and *calb2b* MOs targeted the exon III/intron III and exon II/intron II splice junction respectively. RT-PCR was performed using a specific set of primers in exons III and IV for *calb2a* mRNA and in exon II and III for *calb2b* mRNA. Targeting the E3/I3 splice junction in *calb2a*, and E2/I2 in *calb2b* should result in abnormal exon splicing leading to a predictably 410–460 bp mRNA variant. Our results of RT-PCR of cDNA from NIC and control MO injected embryos using a set of primer for *calb2a* gene shows a 180-bp product consistent with the size of normally spliced mRNA (Fig. 5a, lane 2 and 3). Whereas in cDNA from combined *calb2a* and *calb2b* MOs injected embryos two bands (180 bp and 416 bp) were observed (Fig. 5a, lane 4 and 5). The RT-PCR amplification of *calb2a* and *calb2b* morphant cDNA with primers for *calb2b* gene, respectively, showed multiple bands of 190 bp and 460 bp when compared with uninjected controls with 190 bp a normal-sized band. We have noted that the intensities of the spliced product in the morphant was dose-dependent, in 0.3 mM concentration the effective band intensities were less in spliced variant products indicating the approximately 30–40% of the reduction in mRNA. However, at higher dose i.e. 0.4 mM the splice products of higher intensities were observed with approximately 60–70% mRNA splicing with successive knockdown of both the genes.

Human *CALB2* mRNA can rescue the defective phenotype caused by *calb2a* and *calb2b* combined knockdown

A highly conserved amino acid sequence, including similar motifs and the domains of CALB2 between human and zebrafish, offers a clue that these proteins may have similar functions. Thus, it was hypothesized that human *CALB2* mRNA injection in the zebrafish can rescue the defective phenotype caused by the *calb2a* and *calb2b* combined knockdown. To test this hypothesis, we have co-injected human *CALB2* mRNA with 0.4 mM cocktail of *calb2a* and *calb2b* MO in zebrafish embryos at one cell stage, embryos were examined at 24 hpf. The co-injection of the human *CALB2* mRNA with the *calb2a* and *calb2b* MO rescued 74.67% of the defective phenotype caused by the injection of the zebrafish *calb2a* and *calb2b* MO (Fig. 6A, B).

Homology model predicts conserved protein structure

We have analyzed the structural conservation of Calb2a and Calb2b protein by predicting the tertiary structure of the protein using homology modeling. We have performed BLAST

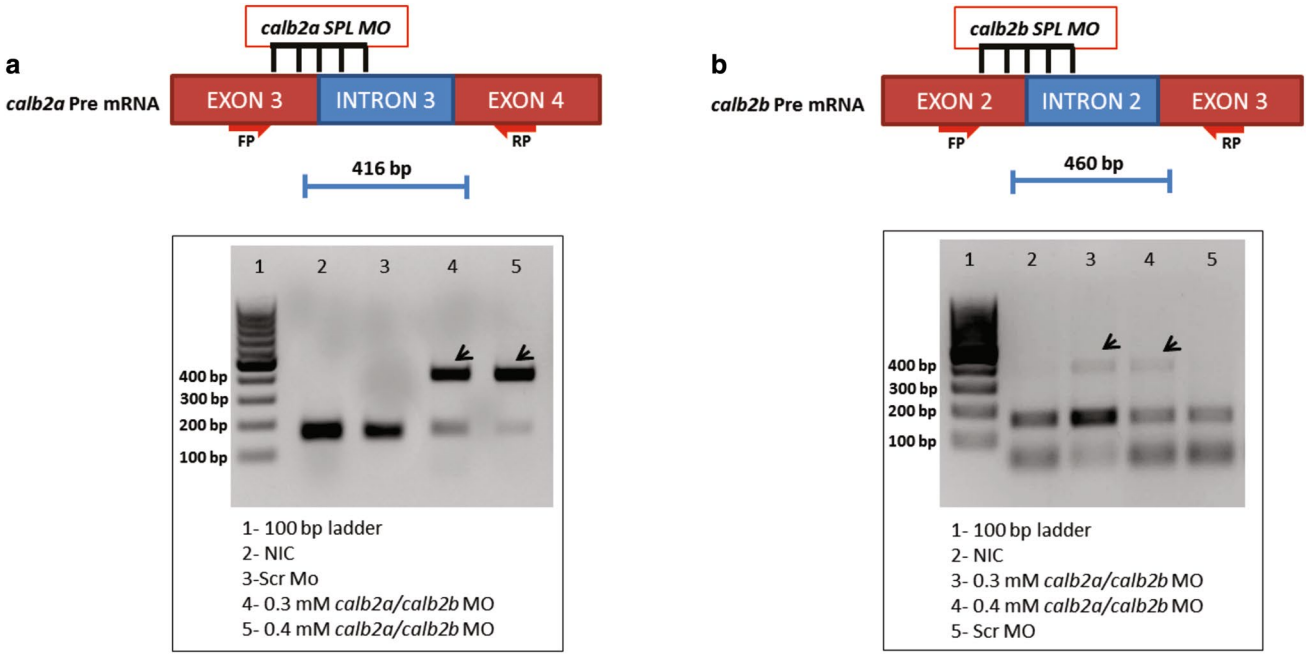

Fig. 5 Knockdown of *calb2a* and *calb2b* leads to aberrant intron retention, **a** cDNA was amplified from RNA isolated from *calb2a* and *calb2b* knockdown morphants and the non-injected control (NIC) embryos. Polymerase chain reaction (PCR) was conducted using the primers in exons 3 and 4 for *calb2a*. The wild-type products (180 bp) and spliced product (416 bp) analyzed on agarose gel, arrowheads indicate the migration of the wild-type and splice variant band in 0.3 mM and 0.4 mM concentration lane 4 and 5 respectively. **b** The cDNA was amplified using primers in exon 2 and exon 3, wild type product (190 bp) and alternatively spliced product (460 bp) analyzed. The arrowheads indicating migration of the wild-type and splice variant products in 0.3 mM and 0.4 mM concentrations (lane 3 and 4 respectively)

against PDB and nine templates for each Calb2a and Calb2b were selected. The selected templates were (PDB id) 1IQ5, 1Y6W, 2BE4, 2F2O, 2G9B, 2N6A, 2WEL, 3WLC, 4BYA, 4E50 for Calb2a and 1CDM, 1GGZ, 1QTX, 1RFJ, 1VRK, 2BE4, 2G9B, 2VAY, 4AQR for Calb2b. The templates had percentage identity between 27–59% for Calb2a and 25–59% for Calb2b and had a low *E* value.

Using EasyModeller 4.0 (Modeller GUI) we have generated 12 homology models for each Calb2a and Calb2b. Apart from this we also have used SWISS-MODEL to generate 6 homology models for each protein and I-TASSER to generate 2 and 1 homology models for Calb2a and Calb2b respectively. We have further validated these models using RC-plot, ERRAT 2, Verify3D, QMEAN score and Dope score in the case of EasyModeller 4.0. RMSD was also performed by aligning the models with the 2G9B template as it belongs to Calb2 of *Rattus norvegicus* and had an identity percentage of 59% for both Calb2a and Calb2b along with the max score of 303 with Calb2a and 287 with Calb2b (Supplementary Table 1). Top models were selected which was CALB2A_SM3 and CLAB2B_SM3 for each protein. The selected model showed 0.732 Å and 0.747 Å RMSD value for Calb2a and Calb2b respectively when aligned with the template 2G9B. A good ERRAT score of 88.353 and 86.667 was obtained for Calb2a and Calb2b respectively. The RC-plot analysis suggested that 89.0% and 91.5% of residues are in the favoured region, Calb2a and Calb2b had a 98.44% and 100% score for verify3D (Fig. 7).

Calb2a and Calb2b predicted structure contains 15 alpha helix structures which together forms a helix-loop-helix (HLH) structural motif which is highly conserved across the Ca^{2+}-binding proteins. We have also superimposed Calb2a and Calb2b selected models with each other and got 0.7 Å RSMD value providing high similarity in structure (Fig. 8a). Also, the protein interactions of both Calb2a and Calb2b were similar when analyzed using STRING (Fig. 8b, c), hence supporting the notion of similar function and interaction which can be performed by one in the absence of other. The helix-loop-helix structure is considered to be important in specific neuronal development (Lee 1997). This HLH structure forms an EF-hand motif which is separated by the flexible Ca^{2+}-binding site. Hence Calb2a and Calb2b of zebrafish belong to a highly conserved protein family belonging to Ca^{2+}-binding family and also help in neural development.

Predicting Ca^{2+}-binding Motif of Calb2a and Calb2b

Calmodulin (CaM) an EF-hand protein which is a multifunctional intermediate calcium-binding messenger protein

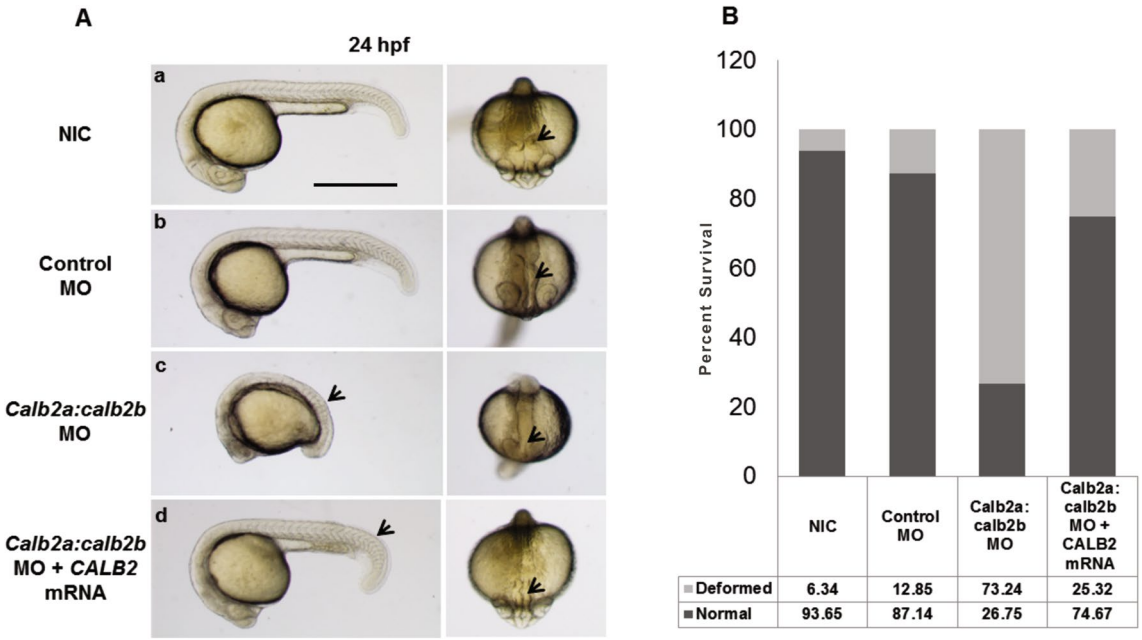

Fig. 6 The *calb2a* and *calb2b* combined knockdown morphant is rescued by the overexpression of human *CALB2* mRNA. (**A**) **a** 24 hpf NIC zebrafish embryo, **b** 24 hpf zebrafish embryo injected with 0.4 mM of 5-mispair specificity control MO, **c** 24 hpf embryo injected with 0.4 mM *calb2a* and *calb2b* cocktail MO, arrowhead showing the disorganized body patterning along with the defective neural folding pattern. **d** Co-injection of 250 pg (picogram) of the full-length human *CALB2* mRNA and 0.4 mM of *calb2a* and *calb2b* cocktail MO, arrowhead showing the normal axial symmetry and the neural tube folding, which shows the partial rescue of the strong mutant phenotype by *CALB2 mRNA* (**B**) Zebrafish morphant rescue statistics. The distribution bar graph shows the phenotypic penetrance of the *calb2a* and *calb2b* MO cocktail, microinjection of the 0.4 mM of MO gives the 73.24% phenotypes. Co-injection of the 250 pg *CALB2* mRNA along with the 0.4 mM MO cocktail leads to the 74.67% rescue of the phenotypes

expressed in all eukaryotic cells. These proteins have flexible EF-hand motif with 4 Ca^{2+}-binding sites present between the loops. These domains are conserved across species and hence we have tried to find these motifs for Calb2a and Calb2b.

COACH was used to predict protein–ligand binding site prediction. It uses TM-SITE and S-SITE (2 comparative analysis) to select the ligand binding templates and further combining it with the results of FINDSITE, COFACTOR and ConCavity to predict the binding site of the protein. The selected homology model of Calb2a and Calb2b was used for the binding site prediction using server-based COACH.

We have found three major binding sites in Calb2a and Calb2b for calcium ion. Predicted binding sites for Calb2a were binding 1–29, 31, 32, 33, 35, 40 which had hydrogen interaction with 29Asp, 31Asp, 33 Asn, 35Tyr and 37Glu in which 31Asp and 33Asn had bonding with all three Ca^{2+}. 31Asp forms bond (OD2 atom) at 2.52 Å with Ca-1, 3.15 Å with Ca-2 and 3.0 Å with Ca-3 ions, whereas 33ASn forms bond (ND2 Atom) at 2,34 Å with Ca-1, 2.42 Å with Ca-2 along with 2.57 Å (ND2 Atom) and 3.19 Å (N atom) with Ca-3 ions.The 35Tyr and 29Asp forms bonding with only 2 calcium ions. 35Tyr forms bonds (O atom) at 3.11 Å with Ca-1asd 2.78 Å with Ca-2ion and 29Asp had bonds (OD2 atom)at 2.84 Å with Ca-2 and 2.83 Å with Ca-3 ion. 37Glu forms a single bond (N atom) with at 3.17 Å with Ca-1 ion (Fig. 9a, a′). The next binding site was binding 2—112, 114, 116, 118, 123 which had three Ca^{2+} ligand bonds with 112Asp and single hydrogen bonding with 118Phe (O atom) at 3,22 Å with Ca-2 and 113Thr (OG1 atom) at 2.29 Å with Ca-1 (Fig. 9b, b′). The last predicted binding site for Calb2a was binding 3—200, 202, 204, 206, 211 which has a total of six Ca^{2+} in the pocket. 206Tyr forms hydrogen bonding with all the six calcium atoms (O atom) at a distance of 1,93 Å (Ca-1), 2.21 Å (Ca-2), 1.94 Å (Ca-3), 2,12 Å (Ca-4), 2.20 Å (Ca-5) and 2.55 Å (Ca-6) whereas 200Asp has hydrogen bonding with three Ca^{2+}(OD1 atom) at 3.13 Å (Ca-1), 2.51 Å (Ca-2) and 2.53 Å (Ca-3). 202Asp has only one hydrogen bond with (OD2 atom) Ca-6 ion at 3.31 Å (Fig. 9c, c′).

The proposed binding sites for Calb2b were binding 1-14, 16, 18, 20, and 25 in which 14Asp forms bonding with both Ca^{2+} (OD1 atom) at a distance of 2.62 Å (Ca-1) and 2.53 Å (Ca-2). 16Asp, 17Gly, 18Asn and 20Cys had only one hydrogen bonding with Ca^{2+} (N atom) at 3.21 Å (Ca-1), 3.12 Å (Ca-1) 3.11 Å (Ca-1) and (O atom) 2.83 Å (Ca-2) respectively (Fig. 9d, d′). The next binding site was predicted at binding 2-191, 193, 195, 197, 202 in which had seven

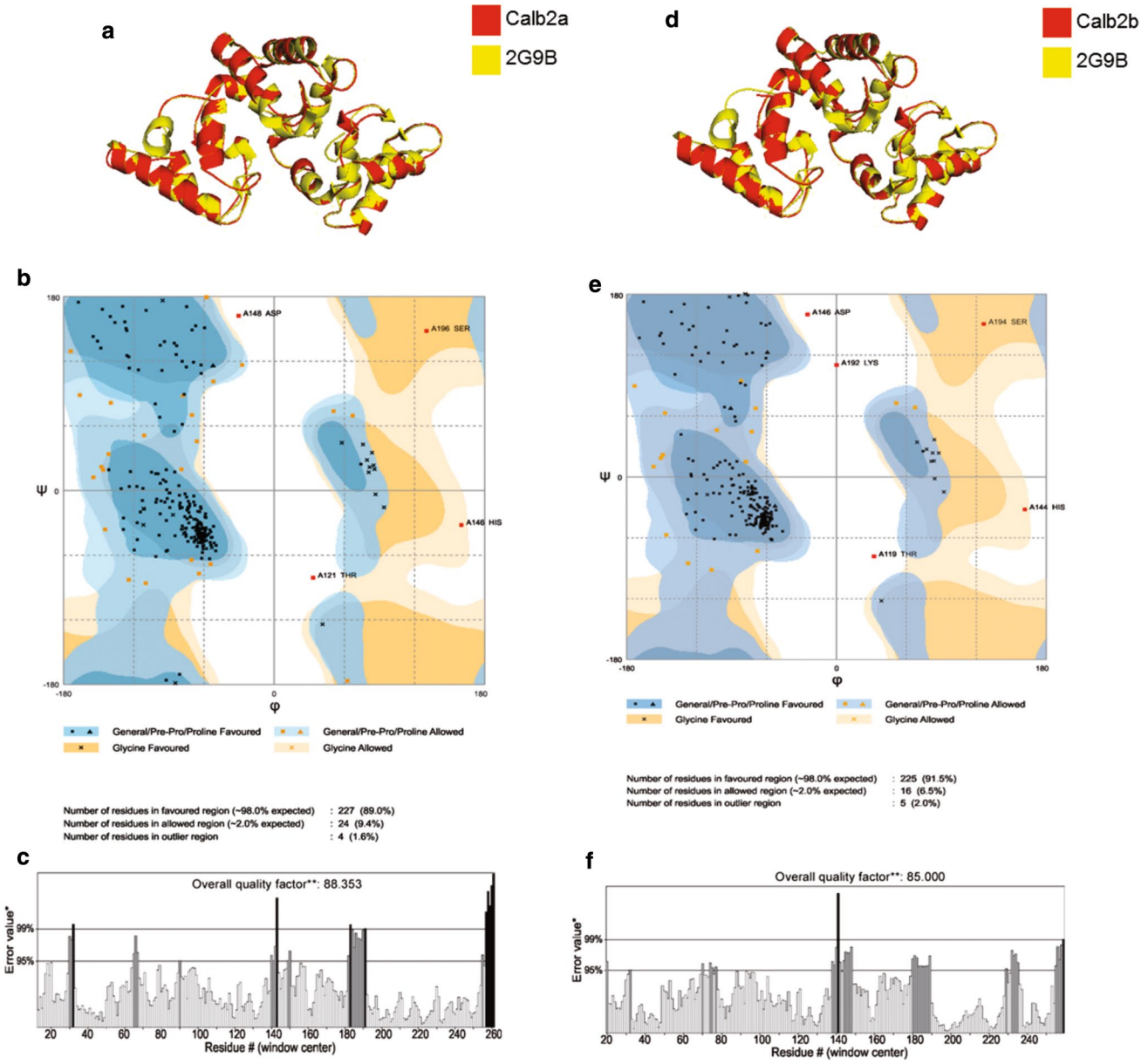

Fig. 7 Validation of homology models of Calb2a and Calb2b. **a** Homology structure of Calb2a (red) overlapping with reference template 2G9B (yellow). **b** Ramachandran plot of selected homology model SM_3 of Calb2a. **c** ERRAT 2 graph for selected homology model SM_3 of Calb2a showing the score of 88.353. **d** Homology structure of Calb2b (red) overlapping with reference template 2G9B (yellow). **e** Ramachandran plot of selected homology model SM_3 of Calb2b. **f** ERRAT2 graph for selected homology model SM_3 of Calb2a showing the score of 85.00

Ca^{2+} binding pockets. Both 191Asp and 197Tyr had hydrogen bonding with five $Ca^{2+}$and 197 Tyr also had a ligand bonding with Ca-2. The hydrogen bonding of 191Asp (OD1 atom) was at 3.05 Å (Ca-1), 3.26 Å (Ca-2), 3.28 Å (Ca-3), 2.44 Å (Ca-4) and 2.48 Å (Ca-6) with the calcium ions whereas 197Tyr had hydrogen bonding (O atom) at 1.87 Å (Ca-1), 2.13 Å (Ca-3), 1.99 Å (Ca-4), 2.17 Å (Ca-6) and 2.09 Å (Ca-7) (Fig. 9e, e′). The last predicted binding site for Calb2b was binding 3—206, 208, 210, 212, 214, 217 which had four Ca^{2+} in the site. Three hydrogen bonds were forms at 2.36 Å (Ca-1), 2.36 Å (Ca-2) and 2.76 Å (Ca-4) with 212Tyr O atom. 214Asp only formed one hydrogen bond (OD2) at 3.33 Å with Ca-1 (Fig. 9f, f′).

The predicted binding sites of both Calb2a and Calb2b were further confirmed using MIB: Metal Ion-Binding Site Prediction and Docking Server (Lin et al. 2016) which gave a score of > 2 for all the predicted sites further confirming the results (Table 1). Other predicted sites were also developed by

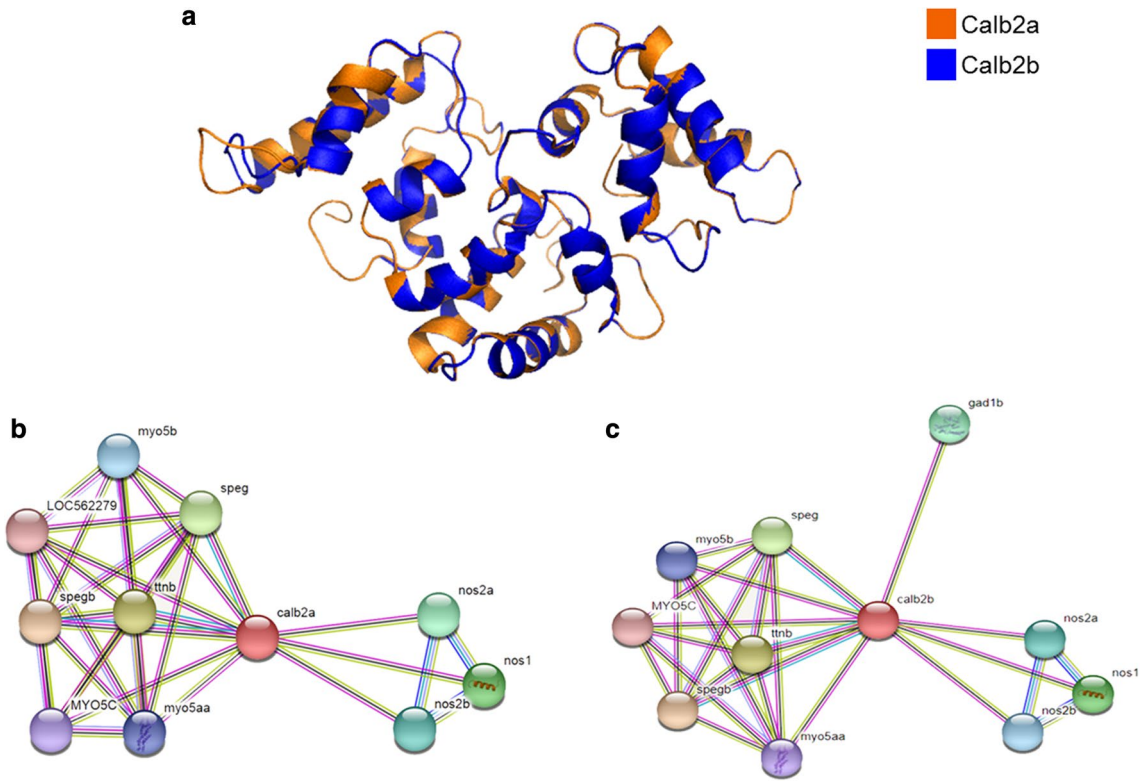

Fig. 8 **a** Overlapping of Calb2a and Calb2b homology model gave an RMSD of 0.7. **b, c** STRING analysis showing homology in gene interaction between *calb2a* and *calb2b*

COACH but had very-low confidence score, hence were not validated further and in the end, we got three major predicted Ca^{2+} binding sites with similar domains in both Calb2a and Calb2b.

Discussion

Calbindin belongs to troponin C super conserved protein family which has a predominant role in calcium transport mechanism and plenty of it is found in neuronal tissues. Calb2 also known as calretinin is present at Chr16q22 in human (Parmentier et al. 1991) and has two copies *calb2a* and *calb2b* in zebrafish at Chr18.21 and Chr7.24, respectively. Our phylogenetic analysis reveals that both Calb2a and Calb2 are part of the common ancestor but got separated long back in the course of evolution, although it could be predicted Calb2 could have been duplicated back in days and adapted in the evolution period. Although they both have almost similar biological function and conserved structure, they might also have new biological function or interaction which might differ from each other and could be related to its neighbouring genes.

Previous studies on CB null mice suggest that CB has evolved as a unique protein, whose function is not entirely backed up by related CaBPs or Ca^{2+}-regulatory mechanisms, whereas the CB knockout mouse develops normally, indicating that the calbindin mutation is not lethal to embryos (Airaksinen et al. 1997). Another study on the CR knockout mice shows that the morphants grow and reproduce normally, with the unaffected mortality rate, and do not present obvious behavioral abnormalities (Schurmans et al. 1997). However, the possibilities are not excluded that the normal levels of both the calcium-binding proteins can fulfill the function of each interchangeably and compensate for their individual loss. To address this, double mutant lacking both *calb2a* and *calb2b* genes may provide further insights.

Using morpholino-based knockdown strategy we have generated combined *calb2a* and *calb2b* morphants along with the double mutants lacking both the genes. Both *calb2a* and *calb2b* MO alone have failed to generate any notable phenotypes; however, the combined knockdown of the *calb2a* and *calb2b* genes resulted in the phenotypes with several developmental defects. Also, the rescue experiment shows that the co-injection of the human *CALB2* mRNA with cocktail of *calb2a* and *calb2b* MO can rescue the defective zebrafish phenotype. Irrespective of exactly how these two genes first appeared, the genetic interaction between the *calb2a* and *calb2b* genes confirms their functional relevance.

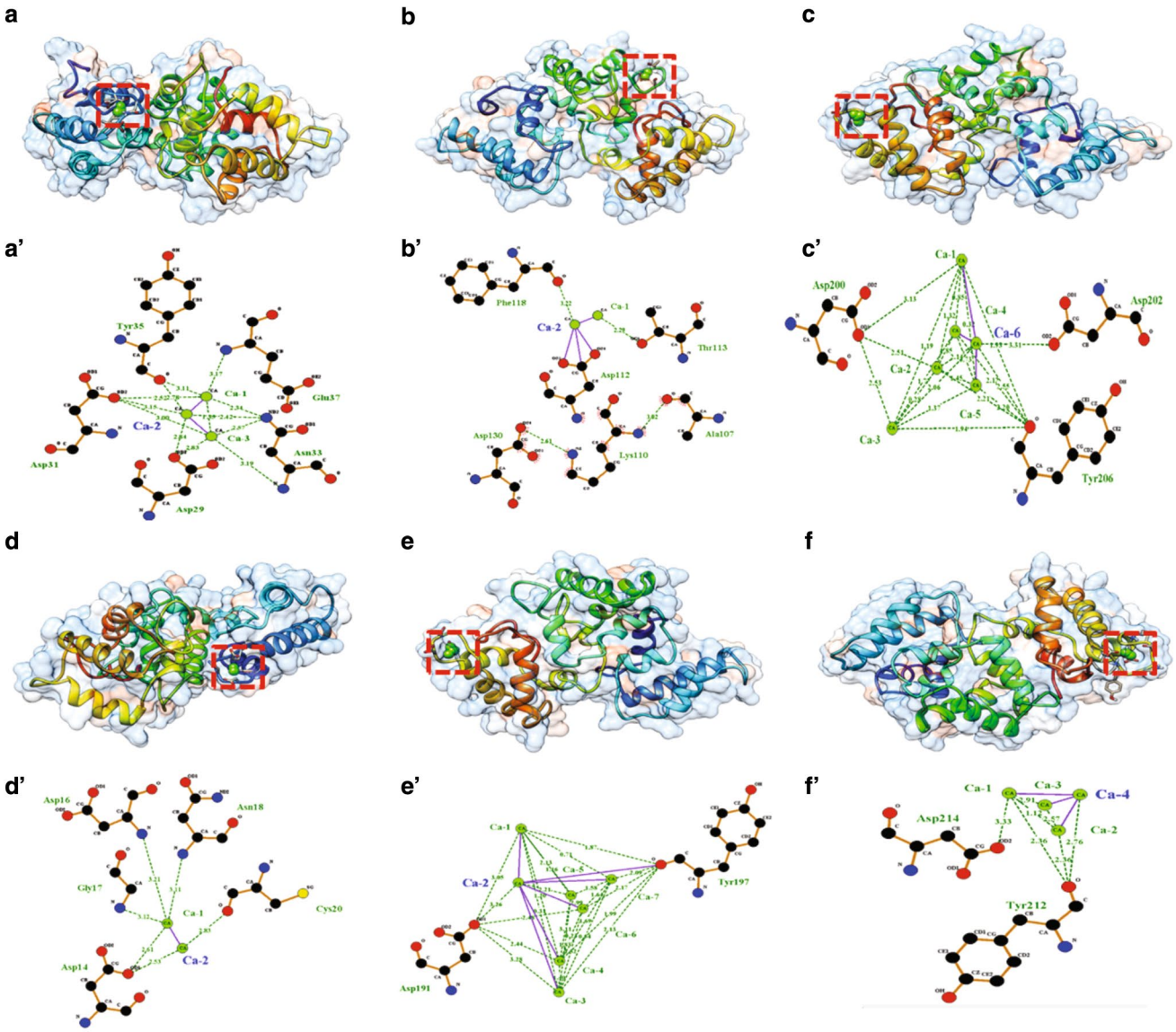

Fig. 9 Docking analysis of Calb2a predicting 3 major Ca^{2+}-binding sites. **a**–**c** Protein structure and the docking site of calcium in Calb2a and d, e and f represent the protein structure and the docking site of calcium in Calb2b. **a′**–**c′** LIGPLOT image providing molecular interaction between the Ca^{2+} and the amino acids in Calb2a and **d′**–**f′** represent the same for Calb2b

Table 1 Docking positions and scores calculated by COACH and MIB

Model	Binding site	COACH C-score	MIB score
Calb2a	29, 31, 32, 33, 35, 40	0.07	2.372
	112, 114, 116, 118, 123	0.15	1.914
	200, 202, 204, 206, 211	0.03	2.472
Calb2b	14, 16, 18, 20,25	0.08	1.933
	191, 193, 195, 197, 202	0.04	2.555
	206, 208, 210, 212, 214, 217	0.10	2.470

A morphological and physiological study conducted on the double mutant provides detailed insights into the commutable functions of these two novel genes. Because *calb2a* and *calb2b* are mainly expressed in specific subpopulations of neurons (Rogers 1987; Bhoyar et al. 2017), precise attentions were taken to the investigation of the central nervous system of the mutant. Our double mutant shows an impaired neural tube folding, which resulted in the disorganized MHB. The MHB region consists of the posteriormost midbrain and the anteriormost hindbrain region, which is thought to give rise to the cerebellum (Kimmel et al. 1995). In zebrafish, MHB maintenance is thought to begin near the five-somite stage, when *wnt1* and *fgf8* expressions become

dependent on the function of *pax2.1* (Lun and Brand 1998). Both of these portions are absent in *calb2a* and *calb2b* combined mutants; this phenotype can be correlated with the acerebellar (ace) mutants (Reifers et al. 1998) which lack the cerebellum and disorganized MHB boundary. These findings clearly suggest that the *calb2a* and *calb2b* genes are directly involved in the maintenance of the MHB region.

As *calb2a* and *calb2b* belong to calcium transport protein, we tried to predict the binding site for calcium and it was observed that multiple sites (3 nos.) were predicted in both *calb2a* and *calb2b* proteins at the similar junctions which supported its function as calcium-transporting ferry (Parmentier et al. 1991) and also helped it determining the important domain for Ca^{2+} binding in Calb2 family. In previous studies it has been observed that there is a conformational change which occurs in the structure of calb2 after binding with Ca^{2+}, which is suspected to be important for calb2 in interacting with other molecules or proteins (Arendt et al. 2013).

The phenotypic consequences of the combined *calb2a* and *calb2b* knockdown are found to be associated with severe hydrocephalus, and defective axial curvature along with the pericardial edema. Several genes are known to be involved in regulating ciliogenesis and cilia function together with the genes that regulate basal body formation and localization, intraflagellar transport, integrity of the axoneme and cytoskeletal organization (Sun et al. 2004a, b; Essner et al. 2005; Kramer-Zucker et al. 2005; Cao et al. 2010; Ravanelli and Klingensmith 2011). Centrin2 (Cetn2) is a small calcium-binding protein which is known for regulation of primary ciliogenesis through controlling CP110 levels (Prosser and Morrison 2015). Interestingly, the ciliary mutants and morphants with defects in diverse ciliary genes display defects including body curvature, hydrocephalus, kidney cysts and left–right asymmetry (Drummond et al. 1998; Sun et al. 2004a, b). Our present results show 84% of the phenotype with severe hydrocephalus along with the defect in axial curvature; this can be related to the *cetn2* where transient knockdown of this gene resulted in the ciliogenesis. These results together suggest the possible role of the *calb2a* and *calb2b* in ciliogenesis; however, to further confirm this detailed study is required.

Responses to sensory stimuli and swimming performance are the extensively studied behaviors in zebrafish embryos and larvae (Brockerhoff et al. 1995; Budick and O'Malley 2000; Bang et al. 2002). Zebrafish display two highly stereotyped touch-evoked escape behaviors: contractions and swimming, during early development (Saint-Amant and Drapeau 1998). Touch-evoked deflation begins at 21 hpf and is characterized by one to three rapid, alternating contractions of the trunk and tail toward the head in response to tactile stimuli delivered along the body axis. Combined knockdown *calb2a* and *calb2b* shows a phenotype with a defect in any responses to the mechanical stimuli and impaired swimming performance. Furthermore, NIC embryos responded to touch at 5 dpf with swimming. Thus, *calb2a* and *calb2b* appear to be essential for touch-evoked escape behaviors during the development as it belongs to calcium pooling protein and in the absence of these proteins the Ca^{2+} pool is reduced further affecting the synaptic plasticity in the neurons leading to negligible sensory behavior (Zündorf and Georg 2011).

Acknowledgements This work was supported by the fund from the Department of Biotechnology (DBT), Government of India (Project no. BT/PR4688/AAQ/03/585/2012) to AGJ. A donation of Axio Imager A2 (Zeiss) microscope by Alexander von Humboldt Foundation, Germany to AGJ, used for the photomicrography, is sincerely acknowledged.

Author contributions All authors had full access to all the data in the study and take responsibility for the integrity of the data and the accuracy of the data analysis. Study concept and design: RCB, AGJ, SSB. Acquisition of data: RCB, SSB, AS. Analysis and interpretation of data: RCB, AGJ, AS, GR. Drafting of the manuscript: RCB, AGJ, CP, A.S, GR.

Compliance with ethical standards

Conflict of interest The authors declare that they have no conflicts of interest.

References

Airaksinen MS, Eilers J, Garaschuk O, Thoenen H, Konnerth A, Meyer M (1997) Ataxia and altered dendritic calcium signaling in mice carrying a targeted null mutation of the calbindin D28k gene. Proc Natl AcadSci USA 94:1488–1493

Altschul SF, Madden TL, Schäffer AA, Zhang J, Zhang Z, Miller W, Lipman DJ (1997) Gapped BLAST and PSI-BLAST: a new generation of protein database search programs. Nucleic Acids Res 25:3389–3402

Amores A et al (1998) Zebrafish hox clusters and vertebrate genome evolution. Science 282:1711–1714

Andressen C, Blümcke I, Celio M (1993) Calcium-binding proteins: selective markers of nerve cells. Cell Tissue Res 271:181–208

Arendt O, Schwaller B, Brown EB, Eilers J, Schmidt H (2013) Restricted diffusion of calretinin in cerebellar granule cell dendrites implies Ca^{2+}-dependent interactions via its EF-hand 5 domain. J Physiol 591:3887–3899

Baimbridge K, Miller J (1982) Immunohistochemical localization of calcium-binding protein in the cerebellum, hippocampal formation and olfactory bulb of the rat. Brain Res 245:223–229

Baimbridge K, Celio M, Rogers J (1992) Calcium-binding proteins in the nervous system. Trends Neurosci 15:303–308

Bang P, Yelick P, Malicki J, Sewell W (2002) High-throughput behavioral screening method for detecting auditory response defects in zebrafish. J Neurosci Methods 118:177–187

Benkert P, Tosatto SC, Schomburg D (2008) QMEAN: a comprehensive scoring function for model quality assessment. Proteins 71:261–277

Berdal A et al (1991) Differential expression of calbindin-D 28 kDa in rat incisor ameloblasts throughout enamel development. Anat Rec 230:149–163

Berman H, Westbrook J, Feng Z, Gilliland G, Bhat TN, Weissig H, Shindyalov IN, Bourne PE (2000) The protein data bank. Nucleic Acids Res 28:235–242

Bhoyar RC, Jadhao AG, Sivasubbu S, Singh AR, Sabharwal A, Palande NV, Biswas S (2017) Neuroanatomical demonstration of calbindin 2a- and calbindin 2b-like calcium binding proteins in the early embryonic development of zebrafish: mRNA study. Int J Dev Neurosci 60:26–33

Brand M et al (1996) Mutations affecting development of the midline and general body shape during zebrafish embryogenesis. Development 123:129–142

Brockerhoff SE, Hurley JB, Janssen-Bienhold U, Neuhauss SC, Driever W, Dowling JE (1995) A behavioural screen for isolating zebrafish mutants with visual system defects. Proc Natl Acad Sci USA 92:10545–10549

Bronner F (1990) Intestinal calcium transport: the cellular pathway. Miner Electrolyte Metab 16:94–100

Brown NP, Leroy C, Sander C (1998) MView: a web-compatible database search or multiple alignment viewer. Bioinformatics 14.4:380–381

Budick S, O'Malley D (2000) Locomotor repertoire of the larval zebrafish: swimming, turning and prey capture. J ExpBiol 203:2565–2579

Cao Y, Park A, Sun Z (2010) Intraflagellar transport proteins are essential for cilia formation and for planar cell polarity. J Am Soc Nephrol 21:1326–1333

Castro A, Becerra M, Manso MJ, Anadón R (2006) Calretinin immunoreactivity in the brain of the zebrafish. *Danio rerio*: distribution and comparison with some neuropeptides and neurotransmitter-synthesizing enzymes. II. Midbrain, hindbrain, and rostral spinal cord. J Comp Neurol 494:792–814

Chard P, Bleakman D, Christakos S, Fullmer C, Miller R (1993) Calcium buffering properties of calbindin D28k and parvalbumin in rat sensory neurons. J Physiol 472:341–357

Christakos S, Friedlander E, Frandsen B, Norman (1979) A Studies on the mode of action of calciferol. XIII. Development of a radioimmunoassay for vitamin D-dependent chick intestinal calcium-binding protein and tissue distribution. J Endocrinol 104:1495–1503

Colovos C, Yeates T (1993) Verification of protein structures: patterns of non-bonded atomic interactions. Protein Sci 2:1511–1519

Deshpande K, Jadhao A (2015) Calcium binding protein calretinin (29kD) localization in the forebrain of the cichlid fish: an immunohistochemical study. Gen Comp Endocrinol 220:93–97

Drummond I et al (1998) Early development of the zebrafish pronephros and analysis of mutations affecting pronephric function. Development 125:4655–4667

Eckfeldt C et al (2005) Functional analysis of human hematopoietic stem cell gene expression using zebrafish. PLoS Biol 3(8):e254

Essner JJ, Amack JD, Nyholm MK, Harris EB, Yost HJ (2005) Kupffers vesicle is a ciliated organ of asymmetry in the zebrafish embryo that initiates left-right development of the brain, heart and gut. Development 132:1247–1260

Fishman M (1999) Zebrafish genetics: the enigma of arrival. Proc Natl Acad Sci USA 96:10554–10556

Heizmann C, Hunzlker W (1991) Intracellular calcium-binding proteins: more sites than insights. Trends Biochem Sci 16:98–103

Hermanson S, Davidson AE, Sivasubbu S, Balciunas D, Ekker SC (2004) Sleeping beauty transposon for efficient gene delivery. Methods Cell Biol 349–362

Hyatt T, Ekker S (1999) Vectors and techniques for ectopic gene expression in zebrafish. Methods Cell Biol 59:117–126

Jadhao A, Deshpande K (2014) Sexually dimorphic distribution of calcium-binding protein, calretinin in the preoptic area of the freshwater catfish, *Clarias batrachus*. Neurosci Lett 579:86–91

Jadhao A, Malz C (2007) Localization of calcium binding protein (Calretinin, 29 kD) in the brain and pituitary gland of the teleost fish: an Immunohistochemical study. Neurosci Res 59:265–276

Jaillon O et al (2004) Genome duplication in the teleost fish Tetraodon nigroviridis reveals the early vertebrate proto-karyotype. Nature 431:946–957

Jande S, Maler L, Lawson D (1981a) Immunohistochemical mapping of vitamin D-dependent calcium binding protein in brain. Nature 294:765–767

Jande S, Toinal S, Lawson D (1981b) Immunohistochemical localization of vitamin D-dependent calcium-binding protein in duodenum, kidney, uterus and cerebellum of chickens. Histochemistry 71:99–116

Karlsson J, Von Hofsten J, Olsson P (2001) Generating transparent zebrafish: a refined method to improve detection of gene expression during embryonic development. Mar Biotechnol 3:522–527

Kimmel CB, Ballard W, Kimmel S, Ullmann B, Schilling T (1995) Stages of embryonic development of the zebrafish. Dev Dyn 203:253–310

Kramer-Zucker AG, Olale F, Haycraft CJ, Yoder BK, Schier AF, Drummond IA (2005) Cilia-driven fluid flow in the zebrafish pronephros, brain and Kupffer's vesicle is required for normal organogenesis. Development 132:1907–1921

Kuntal BK, Aparoy P, Reddanna P (2010) EasyModeller: a graphical interface to MODELLER. BMC Res Notes 3:226–230

Lan C, Laurenson S, Copp BR, Cattin PM, Love DR (2007) Whole organism approaches to chemical genomics: the promising role of zebrafish (*Danio rerio*). Expert Opin Drug Discov 2:1389–1401

Lee JE (1997) Basic helix–loop–helix genes in neural development. Curr Opin Neurobiol 7:13–20

Letunic I, Bork P (2016) Interactive tree of life (iTOL) v3: an online tool for the display and annotation of phylogenetic and other trees. Nucleic Acids Res 44:242–245

Levanti MB, Montalbano G, Laurà R, Ciriaco E, Cobo T, García-Suarez O, Germanà A, Vega JA (2007) Calretinin in the peripheral nervous system of the adult zebrafish. J Anat 212:67–71

Lin YF, Cheng CW, Shih CS, Hwang JK, Yu CS, Lu CH (2016) MIB: metal ion-binding site prediction and docking server. J Chem Inf Model 56(12):2287–2291

Lledo PM, Somasundaram B, Morton AJ, Emson PC, Mason WT (1992) Stable transfection of calbindin-D28k into the GH3 cell line alters calcium currents and intracellular calcium homeostasis. Neuron 9:943–954

Lovell S, Davis I, Arendall W, de Bakker P, Word J, Prisant M, Richardson J, Richardson D (2003) Structure validation by C-alphageometry: phi, psi and C-beta deviation. Proteins 50:437–450

Lun K, Brand MA (1998) Series of no isthmus (noi) alleles of the zebrafish pax2.1 gene reveals multiple signaling events in development of the midbrain-hindbrain boundary. Development 125:3049–3062

Lüthy R, Bowie JU, Eisenberg D (1992) Assessment of protein models with three-dimensional profiles. Nature 5:83–85

Moews P, Kretsinger R (1975) Refinement of the structure of carp muscle calcium-binding parvalbumin by model building and difference Fourier analysis. J Mol Biol 91:201–225

Morcos P (2007) Achieving targeted and quantifiable alteration of mRNA splicing with Morpholino oligos. Biochem Biophys Res Commun 358:521–527

Nasevicius A, Ekker S (2000) Effective targeted gene 'knockdown' in zebrafish. Nat Genet 26:216–220

Nemere I, Leathers V, Thompson B, Luben R, Norman A (1991) Redistribution of calbindin-D28k in chick intestine in response to calcium transport. J Endocrinol 129:2972–2984

Parmentier M, Passage E, Vassart G, Mattei MG (1991) The human calbindin D28k (CALB1) and calretinin (CALB2) genes are located at 8q21. 3 → q22.1 and 16q22 → q23, respectively,

suggesting a common duplication with the carbonic anhydrase isozyme loci. Cytogenet Genome Res 57(1):41–43
Patowary A et al (2013) A sequence-based variation map of zebrafish. Zebrafish 10:15–20
Persechini A, Moncrief N, Kretsinger R (1989) The EF-hand family of calcium-modulated proteins. Trends Neurosci 12:462–467
Pickart M et al (2006) Genome-wide reverse genetics framework to identify novel functions of the vertebrate secretome. PLoS One 1(1):e104
Postlethwait J et al (1998) Vertebrate genome evolution and the zebrafish gene map. Nat Genet 18:345–349
Prosser S, Morrison C (2015) Centrin2 regulates CP110 removal in primary cilium formation. J Cell Biol 208:693–701
Ravanelli A, Klingensmith J (2011) The actin nucleator Cordon-bleu is required for development of motile cilia in zebrafish. Dev Biol 350:101–111
Reifers F, Böhli H, Walsh EC, Crossley PH, Stainier DY, Brand M (1998) Fgf8 is mutated in zebrafish acerebellar (ace) mutants and is required for maintenance of midbrain-hindbrain boundary development and somitogenesis. Development 125:2381–2395
Roberts W (1993) Spatial calcium buffering in saccular hair cells. Nature 363:74–76
Rogers J (1987) Calretinin: a gene for a novel calcium-binding protein expressed principally in neurons. J Cell Biol 105:1343–1353
Saint-Amant L, Drapeau P (1998) Time course of the development of motor behaviors in the zebrafish embryo. J Neurobiol 37:622–632
Schurmans S et al (1997) Impaired LTP induction in the dentate gyrus of calretinin deficient mice. Proc Natl Acad Sci USA 94:10415–10420
Schwede T, Kopp J, Guex N, Peitsch MC (2003) SWISS-MODEL: an automated protein homology-modeling server. Nucleic Acids Res 31:3381–3385
Sievers F, Wilm A, Dineen D et al (2011) Fast, scalable generation of high-quality protein multiple sequence alignments using Clustal Omega. Mol Syst Biol 7:539
Summerton J (1999) Morpholino antisense oligomers: the case for an RNase H-independent structural type. Biochim Biophys Acta 1489:141–158
Sun Z et al (2004a) A genetic screen in zebrafish identifies cilia genes as a principal cause of cystic kidney. Development 131:4085–4093
Sun Z, Amsterdam A, Pazour GJ, Cole DG, Miller MS, Hopkins N (2004b) A genetic screen in zebrafish identifies cilia genes as a principal cause of cystic kidney. Development 131:4085–4093
Szklarczyk D et al (2015) STRING v10: protein–protein interaction networks, integrated over the tree of life. Nucleic Acids Res 43:447–452
UniProt Consortium (2016) UniProt: the universal protein knowledgebase. Nucleic Acids Res 45.D1: D158–D169
Wallace AC, Roman AL, Janet MT (1995) LIGPLOT: a program to generate schematic diagrams of protein–ligand interactions. Protein Eng Des Sel 8.2:127–134
Webb B, Andrej S (2014) Protein structure modeling with MODELLER. Protein structure prediction. Humana Press, Totowa, pp 1–15
Westerfield M (2000) The Zebrafish Book. A guide for the laboratory use of zebrafish (*Danio rerio*). University of Oregon Press, Eugene
Westerfield M (2007) The zebrafish Book: a guide for the laboratory use of zebrafish (*Danio rerio*). Printed by the University of Oregon Press, Eugene
Yang J, Roy A, Zhang Y (2013a) Protein–ligand binding site recognition using complementary binding-specific substructure comparison and sequence profile alignment. Bioinformatics 29:2588–2595
Yang J, Roy A, Zhang Y (2013b) BioLiP: a semi-manually curated database for biologically relevant ligand–protein interactions. Nucleic Acids Res 41:1096–1103
Yokoi H, Yan YL, Miller MR, BreMiller RA, Catchen JM, Johnson EA, Postlethwait JH (2009) Expression profiling of zebrafish sox9 mutants reveals that Sox9 is required for retinal differentiation. Dev Biol 329:1–15
Zhang Y (2008) I-TASSER server for protein 3D structure prediction. BMC Bioinformatics 9:40
Zündorf G, Georg R (2011) Calcium dysregulation and homeostasis of neural calcium in the molecular mechanisms of neurodegenerative diseases provide multiple targets for neuroprotection. Antioxid Redox Signal 14.7:1275–1288